Fluorescence property of photosystem II protein complexes bound to a gold nanoparticle

Kazuki Tahara,[a] Ahmed Mohamed,[b] Kousuke Kawahara,[a] Ryo Nagao,[a] Yuki Kato,[a] Hiroshi Fukumura,[b] Yutaka Shibata,[b] and Takumi Noguchi*[a]

[a]*Division of Material Science, Graduate School of Science, Nagoya University, Furo-cho, Chikusa-ku, Nagoya, 464-8602, Japan*

[b]*Department of Chemistry, Graduate School of Science, Tohoku University, Aramaki Aza Aoba, Aoba-Ku, Sendai 980-8578, Japan.*

**corresponding author*:

Takumi Noguchi

E-mail: tnoguchi@bio.phys.nagoya-u.ac.jp.

Abstract:

Development of an efficient photoanode system for water oxidation is a key to the success of artificial photosynthesis. We previously assembled photosystem II (PSII) proteins, which are an efficient natural photocatalyst for water oxidation, on a gold nanoparticle (GNP) to prepare a PSII-GNP conjugate as an anode system in a light-driven water-splitting nano-device (Noji et al., *J. Phys. Chem. Lett.* 2011, **2**, 2448-2452). In this study, we characterized the fluorescence property of the PSII-GNP conjugate by static and time-resolved fluorescence measurements, and compared with that of free PSII proteins. It was shown that in a static fluorescence spectrum measured at 77 K, the amplitude of a major peak at 683 nm was significantly reduced and a red shoulder at 693 nm disappeared in PSII-GNP. Time-resolved fluorescence measurements showed that picosecond components at 683 nm decayed faster by factors of 1.4-2.1 in PSII-GNP than in free PSII, explaining the observed quenching of the major fluorescence peak. In addition, a nanosecond-decay component arising from a 'red chlorophyll' at 693 nm was lost in time-resolved fluorescence of PSII-GNP, probably due to a structural perturbation of this chlorophyll by interaction with GNP. In consistent with these fluorescence properties, degradation of PSII during strong-light illumination was two times slower in PSII-GNP than in free PSII. The enhanced durability of PSII is an advantageous property of the PSII-GNP conjugate in the development of an artificial photosynthesis device.

Introduction

Efficient utilization of solar energy is essential for addressing the energy and environmental crisis that humankind faces today. In photosynthesis performed by plants and cyanobacteria, electrons extracted from water using solar energy are finally incorporated into CO_2 to synthesize sugars as storable chemical energy.[1-3] Artificial photosynthesis mimics the principle of natural photosynthesis; water is oxidized on a photo-anode and abstracted electrons are used to produce chemical fuels such as H_2 and methanol on a photo-cathode.[4-8] Here, water functions as a common electron donor in both natural and artificial photosynthesis.

One approach to develop efficient artificial photosynthesis systems is utilizing natural photosynthetic proteins, which originally have high quantum efficiencies, and combining them with artificial catalysts in construction of bio-hybrid systems.[9-14] Various photosynthetic proteins including photosystem I (PSI),[15-25] photosystem II (PSII),[26-31] and bacterial reaction centers[32-37] have been attached on metal surfaces or electrodes, where some of them provided photocurrent. Of particular importance is the application of PSII, which is a significantly efficient natural water-oxidizing enzyme,[38-43] because the development of efficient water-oxidizing catalysts is a bottleneck in artificial photosynthesis researches.[44-46]

Previously, we assembled isolated PSII core complexes from the thermophilic cyanobacterium *Thermosynechococcus elongatus* on a gold nanoparticle (GNP) with a 20-nm diameter and produced PSII-GNP conjugates to produce a bio-hybrid anode system aiming at the development of light-driven water-splitting nano-device (Fig.

1A).[47] In this PSII-GNP conjugate, four or five PSII dimers were bound to a single GNP. It was shown that the PSII protein was not denatured on a GNP and provided an O_2-evolution activity with the same level as isolated free PSII under the same buffer conditions.[47] For further development of a water-splitting device by combination with a hydrogen-producing cathode, it is necessary to study the properties of the excited states of antenna chlorophylls (Chls) in the PSII-GNP conjugate, because the optical properties of molecules located near metal nanoparticles are often modified by plasmonic effects.[48-54] Indeed, many studies have observed drastic changes in absorption and fluorescence intensities of photosynthetic proteins by plasmonic interactions with metal nanoparticles or nanostructures.[22,25,55-60]

In this study, we have investigated the fluorescence property of the PSII-GNP conjugates in comparison with free PSII complexes using static and time-resolved fluorescence measurements. The results showed that fluorescence of PSII was significantly quenched by binding on a GNP, which is caused by accelerated decays of the excited singlet states of Chls and the loss of the 'red Chl' as an energy sink. In addition, it was shown that the binding of PSII to a GNP enhanced its durability under strong-light illumination.

Experimental

Preparation of PSII-GNP conjugates

PSII core complexes from *T. elongatus*, in which the C-terminus of the CP47 subunit was histidine tagged,[61] were isolated following the method described

previously.[62] The core complexes were then washed with a buffer containing 50 mM 2-(*N*-morpholino)ethanesulfonic acid (Mes)-NaOH (pH 6.0), 10 mM $MgCl_2$, 5 mM $CaCl_2$, and 0.06% *n*-dodecyl-β-D-maltoside (DM) (buffer A) by ultrafiltration (Vivaspin 500; 100 kDa MWCO; Sartorius Stedim).

PSII-GNP conjugates were prepared by the method by Noji et al.[47] with some modifications. An aqueous GNP (20-nm diameter) solution (final 1.0 nM) was mixed with 3,3'-dithiobis[*N*-(5-amino-5-carboxypentyl)-propionamide-*N*', *N*'-diaceticacid] dihydrochloride (dithiobis(C_2-NTA)) (final 0.1 mM) and 0.06% DM, and the obtained C_2-NTA-GNP was washed twice with a 10 mM NaH_2PO_4/NaOH buffer (pH 7.0) containing 0.06% DM and 1 M betaine (buffer B) by centrifugation (11,900 G, 30 min, 4 °C). The C_2-NTA-GNP was then suspended in buffer B in the presence of 30 μM $NiCl_2$ (buffer C) to obtain Ni-NTA-GNP, which was washed with buffer C by centrifugation (6,000 G, 60 min, 4 °C) and then resuspended in buffer B containing 30 μM $CaCl_2$ (3.0 nM GNP). An aliquot (4.23 μL) of the His-tagged PSII complexes (1.16 mg Chl/mL) suspended in buffer A were mixed with 2 mL of the Ni-NTA-GNP solution (PSII : GNP = 25 : 1), and the mixture was diluted with 8 mL of buffer B containing 1 mM $CaCl_2$ (buffer D). The obtained PSII-GNP conjugates were washed three times with buffer D by centrifugation (11,900 G, 35 min, 4 °C). The concentration of PSII in free PSII and PSII-GNP samples was estimated as a Chl concentration from the absorbance at 665 nm (Q_y peak) of a Chl extract with methanol (ε = 71.43 $mM^{-1}cm^{-1}$).[63]

UV-Vis absorption measurement

UV-Vis absorption spectra were measured at room temperature using a Shimadzu UV-3100PC spectrophotometer at 2.0 nm resolution. The concentrations of free PSII in buffer A and PSII-GNP in buffer D were both 292 ng Chl/mL and a cuvette with a light path length of 1 cm was used.

Static fluorescence measurement

Static fluorescence spectra were measured at 77 K using JASCO FP-6500 fluorescence spectrophotometer with an excitation wavelength of 430 nm (5 nm resolution) at a fluorescence resolution of 3 nm. Samples of free PSII in buffer A and PSII-GNP in buffer D, which were mixed with glycerol (10% V/V) (final concentrations: 11-44 ng Chl/mL), were placed in a glass tube with a diameter of 4 mm in a liquid-nitrogen dewar. Note that the fluorescence property (intensity and band shape) of free PSII was virtually unchanged when it was suspended in buffer D.

Time-resolved fluorescence measurement

Time-resolved fluorescence measurements were performed using a picosecond streak camera system (C10627, Hamamatsu Photonics Inc., Hamamatsu) as described previously.[63] Samples of free PSII in buffer A (final concentration: 15 μg Chl/mL) and PSII-GNP in buffer D (final concentration: 6.4 μg Chl/mL), which were mixed with glycerol (final: 67% V/V), were set in a cell with an optical pass length of 2 mm and cooled to 77 K in a liquid-nitrogen dewar. The sample was excited by a pulse at 430 nm

from a Ti-sapphire laser (MaiTai, Spectra-Physics, Mountain View) with a repetition rate of 80 MHz and a pulse width of 110 fs. With a laser power of 20 μW and a typical excitation-spot diameter of 27 μm, the excitation power was about 44 nJ cm^{-2} $pulse^{-1}$. Fluorescence emitted in the same direction as the excitation light was collected and focused into a polychromator with a slit width of 50 μm. The excitation light was cut off by a long-pass filter (Toshiba, Y45). The FWHM of an instrumental response function (IRF), which was fit well by a Gauss function, was 22 and 70 ps for the 1-ns and 5-ns time ranges, respectively. The central wavelength of the polychromator was set to 680 nm, and the spectral resolution was 3.5 nm. Streak images were recorded over a spectral range of approximately 255 nm with intervals of 0.4 nm. The wavelength dependence of the sensitivity of the system was corrected using a standard lamp. The data were accumulated for 1000 s in each measurement for both 1-ns and 5-ns time ranges. For the 1-ns time range, data of four and two measurements were averaged for PSII-GNP and free PSII, respectively. Intensity values were summed every 5 nm for global fitting analysis and calculation of decay associated spectra (DAS).[64,65]

Photobleaching experiments

Free PSII and PSII-GNP samples in buffer D at the same Chl concentration (146 ng Chl/mL) were placed in a cell with an optical path length of 1 cm in a holder, whose temperature was adjusted to 20 °C by circulating water from a constant temperature bath. The sample was illuminated by continuous white light (~700 mW cm^{-2}) from a Xe lamp (Asahispectra, Max-302) through a cold filter (Optical Coatings

Japan). During illumination, bleaching of Chl was monitored by measuring absorption spectra in the Q_y region every 20 min.

Results and Discussion

An absorption spectrum of PSII-GNP conjugates (Fig. 1A) used in the present study is shown in Fig. 1B (red line) together with spectra of free GNPs (green line) and free PSII complexes (blue line). The spectrum of PSII-GNPs, which is virtually identical to that presented in the previous study,[47] showed a large absorption band at 533 nm arising from surface plasmon absorption of GNPs along with small absorption bands of PSII due to the Q_y and Soret transitions at 674 and 437 nm, respectively. The peak position of GNP in PSII-GNP was red-shifted by 8 nm in comparison with free GNP, reflecting the binding of PSII to a GNP surface through Ni-NTA.[47] In contrast, the positions of PSII bands were unchanged by GNP binding (the Q_y region is expanded in the inset of Fig. 1), which was previously argued as evidence for the intactness of PSII in PSII-GNP conjugates.[47] In the inset of Fig. 1, the Q_y band of PSII-GNP after baseline correction (red line) is compared with that of free PSII (blue line) at the same Chl concentration. It was shown that the Qy band intensity was slightly higher in PSII-GNP than in free PSII without any change of the band shape. This slight increase in the absorption intensity can be caused by a weak plasmonic effect of GNP.

In Fig. 2, a static fluorescence spectrum of the PSII-GNP conjugates measured at 77 K with 430-nm excitation (red solid line) is compared with that of free PSII (blue solid line) at the same Chl concentration (44 ng/mL). Two prominent differences were

observed in these spectra. First, the intensity of a major fluorescence band was 4.3 times smaller in PSII-GNP than that in free PSII. Note that the Chl concentration of these samples was low enough to be free from the effect of reabsorption of fluorescence, as shown in a linear correlation between the concentration and the fluorescence intensity (Fig. 2, inset). Second, a shoulder at 693 nm, which is typical of a fluorescence spectrum of PSII core complexes at 77 K,[64-73] was absent in PSII-GNP; this is clearly shown in a normalized fluorescence spectrum of PSII-GNP (red dotted line). It should be noted that the fluorescence excitation spectrum of PSII-GNP did not provide a GNP band, and hence excitation of GNP by the plasmon absorption was not used for fluorescence emission from PSII-GNP.

To understand the reason for the fluorescence quenching and the absence of a 693-nm shoulder in PSII-GNP, we measured time-resolved fluorescence at 77 K by laser pulse excitation at 430 nm (110 fs width). Streak-camera images of measurements in 1-ns and 5-ns time ranges are shown in Fig. 3 (left and right panels, respectively) for free PSII (A) and PSII-GNP (B). Fluorescence intensities at 683 and 693 nm were extracted from the images, and the time courses of the relative intensities were plotted in Fig. 4 (A: free PSII; B: PSII-GNP). It is clear that a fluorescence lifetime is significantly shorter in PSII-GNP than that in free PSII; fluorescence from PSII-GNP decayed completely within 1 ns, whereas that from free PSII needed more than 5 ns to decay. Note that the absolute fluorescence intensities could not be accurately compared between free PSII and PSII-GNP in this time-resolved measurement, because the fluorescence intensity was very sensitive to a subtle change of the position of each

sample in our instrument, and we used relatively high concentrations of PSII samples, where the linearity in the relationship between concentration and fluorescence intensity (Fig. 2, inset) does not hold anymore, to gain enough fluorescence intensities.

For further analysis of the time-resolved data, global fitting was performed for the fluorescence time courses in a wavelength region of 669-712 nm. Both of the 1-ns and 5-ns range data were used for global fitting for free PSII, whereas only the 1-ns range data were enough for PSII-GNP. The fluorescence time courses of free PSII could be fit with four exponentials with time constants of 14 ps, 91 ps, 658 ps, and 3.5 ns, while those of PSII-GNP were fit with three exponentials with 8-ps, 64-ps, and 308-ps time constants (resultant fitting curves at 683 and 693 nm are shown in black lines in Fig. 4). Obtained decay associated spectra (DAS), which represent the wavelength dependence of the amplitudes of individual components, are presented in Fig. 5. Features of these DAS of free PSII core complexes (Fig. 5A) are very similar to those in the previous study using PSII core complexes from *Thermosynechococcus vulcanus*.[65] When a pair of positive and negative bands are observed at shorter and longer wavelengths, respectively, in the DAS of a certain component, it can be interpreted as the presence of energy transfer from Chl with a shorter-wavelength band to that with a longer-wavelength band. The first 14-ps component shows an energy transfer from ~675 nm to ~683 nm, while the components with peaks at 683 nm decay with 91- and 658-ps time constants. The 91-ps decay is partially linked to an energy transfer to ~693 nm, and the component with a peak at 693 nm slowly decays with a 3.5-ns time constant. By contrast, in PSII-GNP, the nanosecond component at ~693 nm is lost, and the

components at ~685 nm decay with 64-ps and 308-ps time constants without energy transfer. The fastest component at 678 nm decays with an 8-ps time constant, but an energy transfer to the redder component seems to be largely suppressed, because only a small negative amplitude was observed around 693 nm. The absence of the slow component at 693 nm in PSII-GNP is consistent with fluorescence spectra obtained by summing up the fluorescence amplitudes in a 5-ns range (Fig. 6); a shoulder at 693 nm in free PSII is absent in PSII-GNP, which is analogous to the static fluorescence spectra (Fig. 2).

Thus, these analyses show that the two decay components having a maximum at 683 nm in free PSII (τ = 91 and 658 ps) both relax faster in PSII-GNP (τ = 64 and 308 ps) by a factor of 1.4-2.1. In these two components, the amplitude of the faster component relative to the slower component is increased in PSII-GNP (Fig. 5). The shorter-wavelength component at 675-678 nm also relaxes faster with a suppressed energy transfer (τ = 14 ps in free PSII to τ = 8 ps in PSII-GNP). These accelerated fluorescence decays should be the reason for the quenching of static fluorescence in PSII-GNP (Fig. 2). The faster decays of the picosecond components may be caused by energy transfer from the lowest singlet excited states of antenna Chls to GNPs. Indeed, many studies have reported fluorescence quenching by energy transfer from dye molecules to metal nanoparticles.[50-54] Electron transfer from the excited state of Chl to a GNP is another possible mechanism of fluorescence quenching,[74,75] but this is less likely because there is no direct contact between Chls and a GNP in PSII-GNP.

In addition to faster decays of the components at 683 nm, the component at 693

nm, which showed the slowest decay with a 3.5-ns time constant, was lost in PSII-GNP. Thus, the reason for the absence of the 693-nm shoulder in the static fluorescence spectrum of PSII-GNP (Fig. 2) is not fluorescence quenching but the loss of the emission around 693 nm from a so-called 'red Chl'. This 'red Chl' has been proposed to be located in the CP47 protein in the PSII complex.[64-73] The most probable candidate is Chl627 (following Chl numbering by Umena et al.[76]), which is ligated by His114 of CP47 on the stromal side of PSII (Fig. 7).[64,65,69,71-73] According to the high-resolution X-ray crystallographic structure of PSII,[76] the conjugated keto C=O group of Chl627 is hydrogen-bonded with Thr5 of the PsbH subunit with a hydrogen-bond distance of 2.7 Å (Fig. 7B), which was suggested to induce a red shift of Q_y absorption.[73] Indeed, a recent study of the ΔPsbH mutant of *Synechocystis* sp. PCC 6803 showed the absence of the ~695 nm shoulder in a fluorescence spectrum.[73] Thus, the loss of the 693-nm fluorescence component in PSII-GNP is most probably attributed to disruption of the hydrogen bond between the keto C=O of Chl627 and PsbH-Thr5. In our PSII complex, a His-tag that is bound to a GNP via Ni-NTA is located at the C-terminus of CP47 on the stromal side of PSII. Chl627 and PsbH-Thr5 are also located on the stromal side, and furthermore the loop region of PsbH near Thr5 is directly exposed to stroma (Fig. 7). It is thus likely that the structure of the PsbH subunit is perturbed by an interaction with GNP and then the hydrogen bond between Thr5 and the keto C=O of Chl627 is disrupted, inducing a blue shift of the Q_y band of this Chl and hence the loss of the emission at 693 nm from the 'red Chl'. It should be noted, however, that such a perturbation of PsbH does not affect the water oxidation activity at the Mn_4CaO_5 cluster,

which is located on the lumenal side of PSII across the membrane (Fig. 7A), as already shown in our previous study in which an O_2-evolution activity was virtually unchanged between PSII-GNP and free PSII.[47] Here, the unchanged O_2-evolution activity even with faster relaxation of the Chl excited states in PSII-GNP is due to saturated incident light used in the O_2-evolution measurement,[47] where excitation energy transfer from antenna Chls to the reaction center is not a rate-limiting process.

From the observed fluoresce quenching and the loss of the 'red Chl' as an energy sink in PSII-GNP, it is expected that the durability of PSII proteins will be enhanced in the PSII-GNP conjugates in comparison with free PSII. This is because degradation of PSII is generally caused by harmful singlet oxygen produced via an excited triplet state of Chl, which is formed by intersystem crossing from the lowest excited singlet state. The rate of degradation of PSII was compared between the free PSII and PSII-GNP samples by monitoring the photo-bleaching of Chl during strong-light illumination (Fig. 8). The result showed that the amplitude of a Chl Q_y band decayed with a single exponential with time constants of 36 and 71 min for free PSII and PSII-GNP, respectively. Thus, degradation of PSII was two times slower in PSII-GNP than in free PSII; in other words, the durability of PSII in the PSII-GNP conjugates was enhanced by a factor of two. This enhanced durability of PSII is an advantageous property of the PSII-GNP conjugate as a water-oxidizing anode for the development of bio-hybrid artificial photosynthesis systems.

Acknowledgements

This study was supported by the Grants-in-Aids for Scientific Research from JSPS (24000018 and 24107003 to T.N. and 15H04356 to Y.S.).

References

1 R. E. Blankenship, *Molecular Mechanisms of Photosynthesis*, 2nd Edition, Wiley-Blackwell, Oxford, UK, 2014.

2 *Photosynthesis: Plastid Biology, Energy Conversion and Carbon Assimilation*, eds. J. J. Eaton-Rye, B. C. Tripathy and T. D. Sharkey, Springer, Dordrecht, The Netherlands, 2012.

3 *Molecular Solar Fuels*, eds. T. Wydrzynski and W. Hillier, Royal Society of Chemistry, Cambridge, UK, 2012.

4 D. Gust, T. A. Moore and A. L. Moore, *Acc. Chem. Res.*, 2009, **42**, 1890–1898.

5 D. G. Nocera, *Acc. Chem. Res.*, 2012, **45**, 767–776.

6 Y. Tachibana, L. Vayssieres and J. R. Durrant, *Nat. Photonics*, 2012, **6**, 511–518.

7 S. Berardi, S. Drouet, L. Francàs, C. Gimbert-Suriñach, M. Guttentag, C.Richmond, T. Stoll and A. Llobet, *Chem. Soc. Rev.*, 2014, **43**, 7501–7519.

8 M. D. Kärkäs, O. Verho, E. V. Johnston and B. Åkermark, *Chem. Rev.*, 2014, **114**, 11863–12001.

9 B. Kandemir, S. Chakraborty, Y. X. Guo and K. L. Bren, *Inorg. Chem.*, 2016, **55**, 467–477.

10 N. Sekar and R. P. Ramasamy, *J. Photochem. Photobiol. C*, 2015, **22**, 19–33.

11 O. Yehezkeli, R. Tel-Vered, D. Michaeli, I. Willner and R. Nechushtai, *Photosynth. Res.*, 2014, **120**, 71–85.

12 M. Kato, J. Z. Zhang, N. Paul and E. Reisner, *Chem. Soc. Rev.*, 2014, **43**, 6485–6497.

13 J. Kargul, J. D. J. Olmos and T. Krupnik, *J. Plant Physiol.*, 2012, **169**, 1639–1653.

14 A. Badura, T. Kothe, W. Schuhmann and M. Rögner, *Energy Environ. Sci.*, 2011, **4**, 3263–3274.

15 J. F. Millsaps, B. D. Bruce, J. W. Lee and E. Greenbaum, *Photochem. Photobiol.*, 2001, **73**, 630–635.

16 I. J. Iwuchukwu, M. Vaughn, N. Myers, H. O'Neill, P. Frymier and B. D. Bruce, *Nat. Nanotechnol.*, 2010, **5**, 73–79.

17 L. M. Utschig, N. M. Dimitrijevic, O. G. Poluektov, S. D. Chemerisov, K. L. Mulfort and D. M. Tiede, *J. Phys. Chem. Lett.*, 2011, **2**, 236–241.

18 R. A. Grimme, C. E. Lubner, D. A. Bryant and J. H. Golbeck, *J. Am. Chem. Soc.*, 2008, **130**, 6308–6309.

19 G. LeBlanc, E. Gizzie, S. Yang, D. E. Cliffel and G. K. Jennings, *Langmuir*, 2014, **30**, 10990–11001.

20 F. Zhao, F. Conzuelo, V. Hartmann, H. Li, M. M. Nowaczyk, N. Plumeré, M. Rögner and W. Schuhmann, *J. Phys. Chem. B*, 2015, **119**, 13726–13731.

21 K. R. Stieger, S. C. Feifel, H. Lokstein and F. Lisdat, *Phys. Chem. Chem. Phys.*, 2014, **16**, 15667–15674.

22 I. Carmeli, I. Lieberman, L. Kraversky, Z. Fan, A. O. Govorov, G. Markovich and

S. Richter, *Nano Lett.*, 2010, **10**, 2069–2074.

23 M. Miyachi, Y. Yamanoi, Y. Shibata, H. Matsumoto, K. Nakazato, M. Konno, K. Ito, Y. Inoue and H. Nishihara, *Chem. Commun.*, 2010, **46**, 2557–2559.

24 M. Brecht, M. Hussels, J. B. Nieder, H. Fang and C. Elsässer, *Chem. Phys.*, 2012, **406**, 15–20.

25 I. Kim, S. L. Bender, J. Hranisavljevic, L. M. Utschig, L. Huang, G. P. Wiederrecht and D. M. Tiede, *Nano Lett.*, 2011, **11**, 3091–3098.

26 J. Maly, J. Krejci, M. Ilie, L. Jakubka, J. Masojídek, R. Pilloton, K. Sameh, P. Steffan, Z. Stryhal and M. Sugiura, *Anal. Bioanal. Chem.*, 2005, **381**, 1558–1567.

27 A. Badura, B. Esper, K. Ataka, C. Grunwald, C. Wöll, J. Kuhlmann, J. Heberle and M. Rögner, *Photochem. Photobiol.*, 2006, **82**, 1385–1390.

28 N. Terasaki, M. Iwai, N. Yamamoto, T. Hiraga, S. Yamada and Y. Inoue, *Thin Solid Films*, 2008, **516**, 2553–2557.

29 M. Vittadello, M. Y. Gorbunov, D. T. Mastrogiovanni, L. S. Wielunski, E. L. Garfunkel, F. Guerrero, D. Kirilovsky, M. Sugiura, A. W. Rutherford, A. Safari and P. G. Falkowski, *ChemSusChem*, 2010, **3**, 471–475.

30 O. Yehezkeli, R. Tel-Vered, J. Wasserman, A. Trifonov, D. Michaeli, R. Nechushtai and I. Willner, *Nat. Commun.*, 2012, **3**, 742.

31 M. Kato, T. Cardona, A. W. Rutherford and E. Reisner, *J. Am. Chem. Soc.*, 2013, **135**, 10610–10613.

32 S. A. Trammell, I. Griva, A. Spano, S. Tsoi, L. M. Tender, J. Schnur and N. Lebedev, *J. Phys. Chem. C*, 2007, **111**, 17122–17130.

33 M.-J. den Hollander, J. G. Magis, P. Fuchsenberger, T. J. Aartsma, M. R. Jones and R. N. Frese, *Langmuir*, 2011, **27**, 10282–10294.

34 V. Bhalla and V. Zazubovich, *Surf. Sci.*, 2012, **606**, 1323–1326.

35 K. Woronowicz, S. Ahmed, A. A. Biradar, A. V. Biradar, D. P. Birnie, T. Asefa and R. A. Niederman, *Photochem. Photobiol.*, 2012, **88**, 1467–1472.

36 M. Kondo, K. Iida, T. Dewa, H. Tanaka, T. Ogawa, S. Nagashima, K. V. P. Nagashima, K. Shimada, H. Hashimoto, A. T. Gardiner, R. J. Cogdell and M. Nango, *Biomacromolecules*, 2012, **13**, 432–438.

37 H. Yaghoubi, Z. Li, D. Jun, E. Lafalce, X. M. Jiang, R. Schlaf, J. T. Beatty and A. Takshi, *J. Phys. Chem. C*, 2014, **118**, 23509–23518.

38 J. P. McEvoy and G. W. Brudvig, *Chem. Rev.*, 2006, **106**, 4455–4483.

39 J. Messinger, T. Noguchi and J. Yano, in *Molecular Solar Fuels*, eds. T. Wydrzynski and W. Hillier, Chapter 7, Royal Society of Chemistry, Cambridge, UK, 2012, pp. 163–207.

40 A. Grundmeier and H. Dau, *Biochim. Biophys. Acta*, 2012, **1817**, 88–105.

41 D. J. Vinyard, G. M. Ananyev and G. C. Dismukes, *Annu. Rev. Biochem.*, 2013, **82**, 577−606.

42 N. Cox and J. Messinger, *Biochim. Biophys. Acta*, 2013, **1827**, 1020–1030.

43 J. Yano and V. Yachandra, *Chem. Rev.*, 2014, **114**, 4175−4205.

44 L. Yang, H. Zhou, T. Fan and D. Zhang, *Phys. Chem. Chem. Phys.*, 2014, **16**, 6810 −6826.

45 K. S. Joya and H. J. M. de Groot, *Int. J. Hydrogen Energy*, 2012, **37**, 8787−8799.

46 W. A. A. Arafa, M. D. Kärkäs, B.-L. Lee, T. Åkermark, R.-Z. Liao, H.-M. Berends, J. Messinger, P. E. M. Siegbahn and B. Åkermark, *Phys. Chem. Chem. Phys.*, 2014, **16**, 11950−11964.

47 T. Noji, H. Suzuki, T. Gotoh, M. Iwai, M. Ikeuchi, T. Tomo and T. Noguchi, *J. Phys. Chem. Lett.*, 2011, **2**, 2448–2452.

48 S. Kühn, U. Håkanson, L. Rogobete and V. Sandoghdar, *Phys. Rev. Lett.*, 2006, **97**, 017402.

49 I. Lieberman, G. Shemer, T. Fried, E. M. Kosower and G. Markovich, *Angew. Chem. Int. Ed.*, 2008, **47**, 4855−4857.

50 P. Anger, P. Bharadwaj and L. Novotny, *Phys. Rev. Lett.*, 2006, **96**, 113002.

51 E. Dulkeith, A. C. Morteani, T. Niedereichholz, T. A. Klar, J. Feldmann, S. A. Levi, F. C. J. M. van Veggel, D. N. Reinhoudt, M. Möller and D. I. Gittins, *Phys. Rev. Lett.*, 2002, **89**, 203002.

52 C. H. Fan, S. Wang, J. W. Hong, G. C. Bazan, K. W. Plaxco and A. J. Heeger, *Proc. Natl. Acad. Sci. U. S. A.*, 2003, **100**, 6297−6301.

53 T. L. Jennings, M. P. Singh and G. F. Strouse, *J. Am. Chem. Soc.*, 2006, **128**, 5462−5467.

54 R. Carminati, J.-J. Greffet, C. Henkel and J. M. Vigoureux, *Opt. Comm.*, 2006, **261**, 368−375.

55 Ł. Bujak, M. Olejnik, T. H. P. Brotosudarmo, M. K. Schmidt, N. Czechowski, D. Piatkowski, J. Aizpurua, R. J. Cogdell, W. Heisse and S. Mackowski, *Phys. Chem. Chem. Phys.*, 2014, **16**, 9015−9022.

56 M. Olejnik, B. Krajnik, D. Kowalska, G. H. Lin and S. Mackowski, *J. Phys.: Condens. Matter*, 2013, **25**, 194103.

57 J. B. Nieder, R. Bittl and M. Brecht, *Angew. Chem. Int. Ed.*, 2010, **49**, 10217−10220.

58 S. R. Beyer, S. Ullrich, S. Kudera, A. T. Gardiner, R. J. Cogdell and J. Köhler, *Nano Lett.*, 2011, **11**. 4897−4901.

59 W. F. Falco, E. R. Botero, E. A. Falcão, E. F. Santiago, V. S. Bagnato and A. R. L. Caires, *J. Photochem. Photobiol. A*, 2011, **225**, 65−71.

60 E. Wientjes, J. Renger, A. G. Curto, R. Cogdell and N. F. van Hulst, *Phys. Chem. Chem. Phys.*, 2014, **16**, 24739−24746.

61 M. Iwai, T. Suzuki, A. Kamiyama, I. Sakurai, N. Dohmae, Y. Inoue and M. Ikeuchi, *Plant Cell Physiol.*, 2010, **51**, 554–560.

62 S. Nakamura, R. Nagao, R. Takahashi and T. Noguchi, *Biochemistry*, 2014, **53**, 3131–3144.

63 R. J. Porra, W. A. Thompson and P. E. Kriedemann, *Biochim. Biophys. Acta*, 1989, **975**, 384–394.

64 A. Mohamed, R. Nagao, T. Noguchi, H. Fukumura and Y. Shibata, *J. Phys. Chem. B*, 2016, **120**, 365–376.

65 Y. Shibata, S. Nishi, K. Kawakami, J.-R. Shen and T. Renger, *J. Am. Chem. Soc.*, 2013, **135**, 6903−6914.

66 R. J. van Dorssen, J. J. Plijter, J. P. Dekker, A. den Ouden, J. Amesz and H. J. van Gorkom, *Biochim. Biophys. Acta*, 1987, **890**, 134−143.

67 E. G. Andrizhiyevskaya, A. Chojnicka, J. A. Bautista, B. A. Diner, R. van Grondelle and J. P. Dekker, *Photosynth. Res.*, 2005, **84**, 173−180.

68 M. Reppert, K. Acharya, B. Neupane and R. Jankowiak, *J. Phys. Chem. B*, 2010, **114**, 11884−11898.

69 F. L. de Weerd, M. A. Palacios, E. G. Andrizhiyevskaya, J. P. Dekker and R. van Grondelle, *Biochemistry*, 2002, **41**, 15224−15233.

70 M. Komura, Y. Shibata and S. Itoh, *Biochim. Biophys. Acta*, 2006, **1757**, 1657−1668.

71 G. Shen and W. F. J. Vermaas, *J. Biol. Chem.*, 1994, **269**, 13904−13910.

72 G. Raszewski and T. Renger, *J. Am. Chem. Soc.*, 2008, **130**, 4431−4446.

73 S. E. D'Haene, R. Sobotka, L. Bučinská, J. P. Dekker and J. Komenda, *Biochim. Biophys. Acta*, 2015, **1847**, 1327−1334.

74 S. Barazzouk, P. V. Kamat and S. Hotchandani, *J. Phys. Chem. B*, 2005, **109**, 716–723.

75 A. M. Queiroz, A. V. Mezacasa, D. E. Graciano, W. F. Falco, J. C. M'Peko, F. E. G Guimarães, T. Lawson, I. Colbeck, S. L. Oliveira and A. R. L. Caires, *Spectrochim. Acta A*, 2016, **168**, 73–77.

76 Y. Umena, K. Kawakami, J.-R. Shen and N. Kamiya, *Nature,* 2011, **473**, 55–60.

Figure Captions

Fig. 1 (A) Schematic structure of a PSII-GNP conjugate. Four to five PSII dimers are bound to single GNP with a diameter of 20 nm.[47] (B) Absorption spectrum of PSII-GNP conjugates (red line) in comparison with spectra of free GNP (green line) and free PSII complexes (blue line). Spectra were measured at room temperature. The spectrum of free PSII was multiplied by 15. The Chl concentration was 292 ng Chl/mL in both the free PSII and PSII-GNP samples. The spectral intensity of free GNP was normalized to that of PSII-GNP at the plasmon absorption band. Inset: The Chl Q_y band of PSII-GNP (red line) after baseline correction in comparison with that of free PSII (blue line).

Fig. 2 Static fluorescence spectra of free PSII complexes (blue line) and PSII-GNP conjugates (red solid line). A normalized spectrum of PSII-GNP, obtained by multiplication of the original spectrum by 4.3, is also shown (red dotted line). Spectra were measured at 77 K with an excitation wavelength of 430 nm. The Chl concentration was 44 ng Chl/mL in both the free PSII and PSII-GNP samples. An inset shows the concentration dependence of the fluorescence intensity of free PSII (blue circles) and PSII-GNP (red circles), showing a linearity at the concentration used for fluorescence measurements.

Fig. 3 Streak-camera image in time-resolved fluorescence measurements for free PSII (A) and PSII-GNP (B) in the 660-720 nm range. The left and right panels show the

results of the measurements of 1-ns and 5-ns time ranges, respectively. The sample was excited with a 430-nm pulse (a pulse width of 110 fs) from a Ti-sapphire laser. The wavelengths of 683 and 693 nm, which are the band positions in the static fluorescence spectra (Fig. 2), are marked by red lines.

Fig. 4 Time courses of fluorescence intensities at 683 (blue line) and 693 (red line) nm for free PSII (A) and PSII-GNP (B). Left and right panels show the data of measurements in 1-ns and 5-ns time ranges, respectively. The fitting curves obtained by global fit analysis, in which both the 1-ns and 5-ns range data were used for free PSII and only the 1-ns range data were used for PSII-GNP, are also shown in black lines.

Fig. 5 Decay associated spectra (DAS) obtained by global fit analysis of time-resolved fluorescence data for free PSII (A) and PSII-GNP (B).

Fig. 6 Fluorescence spectra of free PSII (blue line) and PSII-GNP (red line) as sums of the time-resolved fluorescence data in the 5-ns range. Spectra are normalized at the 684-nm peak.

Fig. 7 (A) Location of Chl627 as a candidate of 'red Chl' in a PSII monomer (red balls). The position of a His tag at the C-terminus of CP47 on the stromal side is also indicated by a red bar. (B) Interaction of Chl627 with CP47 (cyan ribbon) and PsbH (red ribbon). Chl627 is hydrogen bonded with PsbH-Thr5. The structure of the PSII

complex was obtained from the X-ray crystallographic structure at 1.9 Å resolution (PDB entry: 3ARC[76]).

Fig. 8 Photo-bleaching process of free PSII (blue circles) and PSII-GNP (red circles). Free PSII and PSII-GNP samples at the same Chl concentration (146 ng Chl/mL) were illuminated by continuous white light (~700 mW cm^{-2}) at 20 °C, and the intensity change of the Chl Q_y band was monitored.

Figure 1

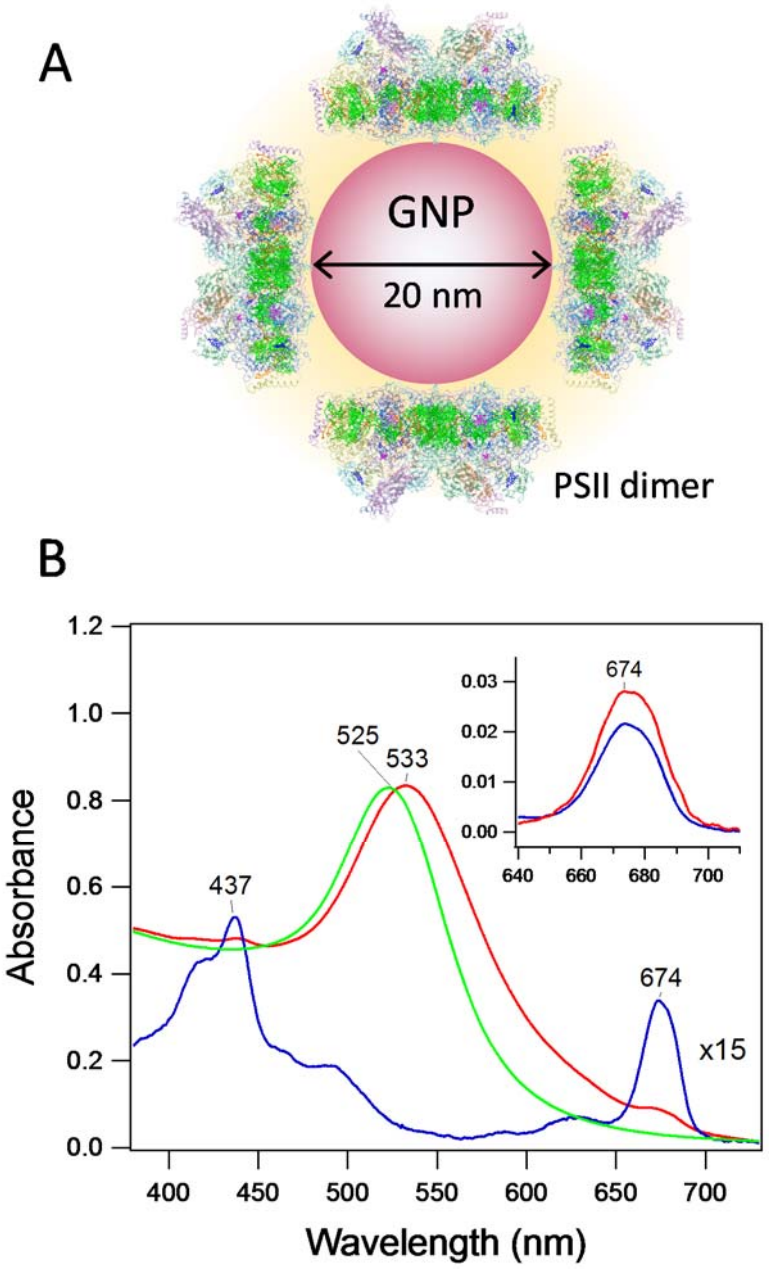
A
GNP
20 nm
PSII dimer
B
Absorbance
Wavelength (nm)
437
525
533
674
x15
674

Figure 2

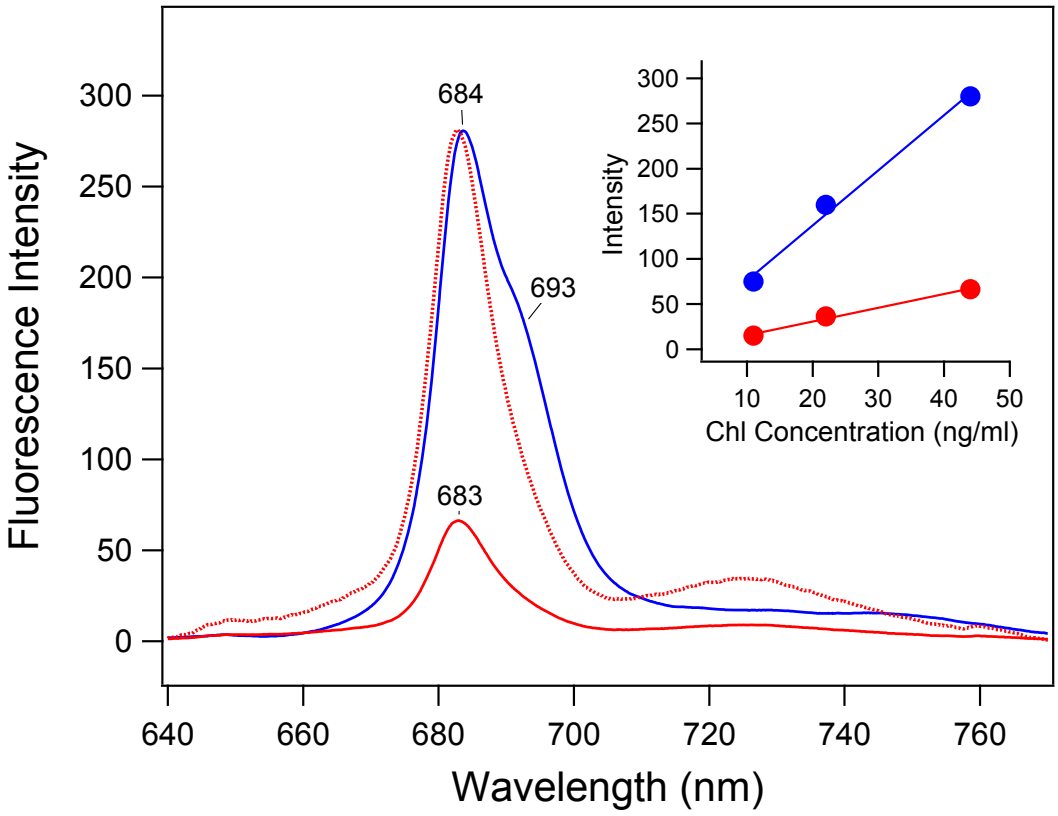
Fluorescence Intensity
300
250
200
150
100
50
0
640
660
680
700
720
740
760
Wavelength (nm)
684
693
683
Intensity
300
250
200
150
100
50
0
10
20
30
40
50
Chl Concentration (ng/ml)

Figure 3

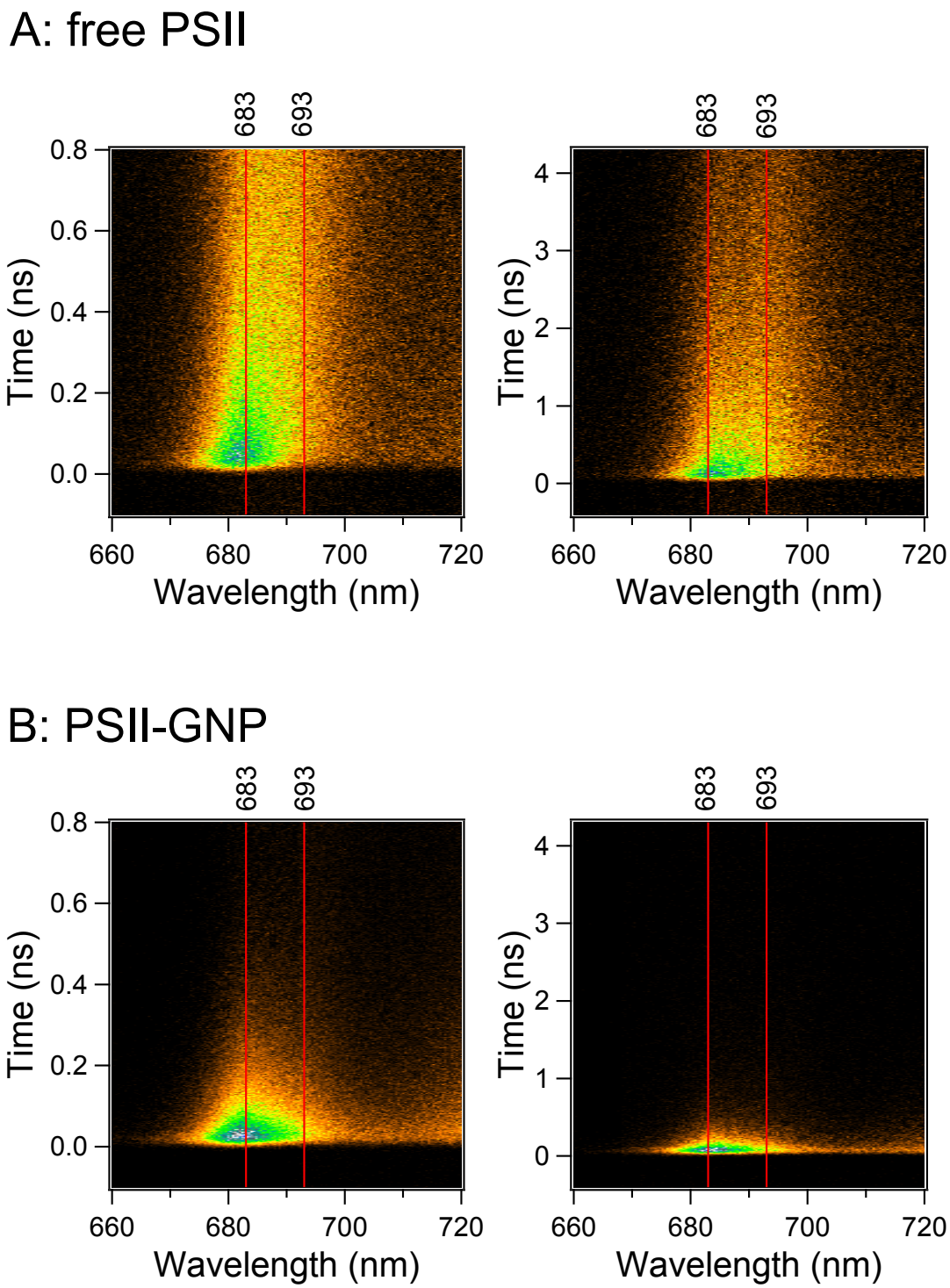

Figure 4

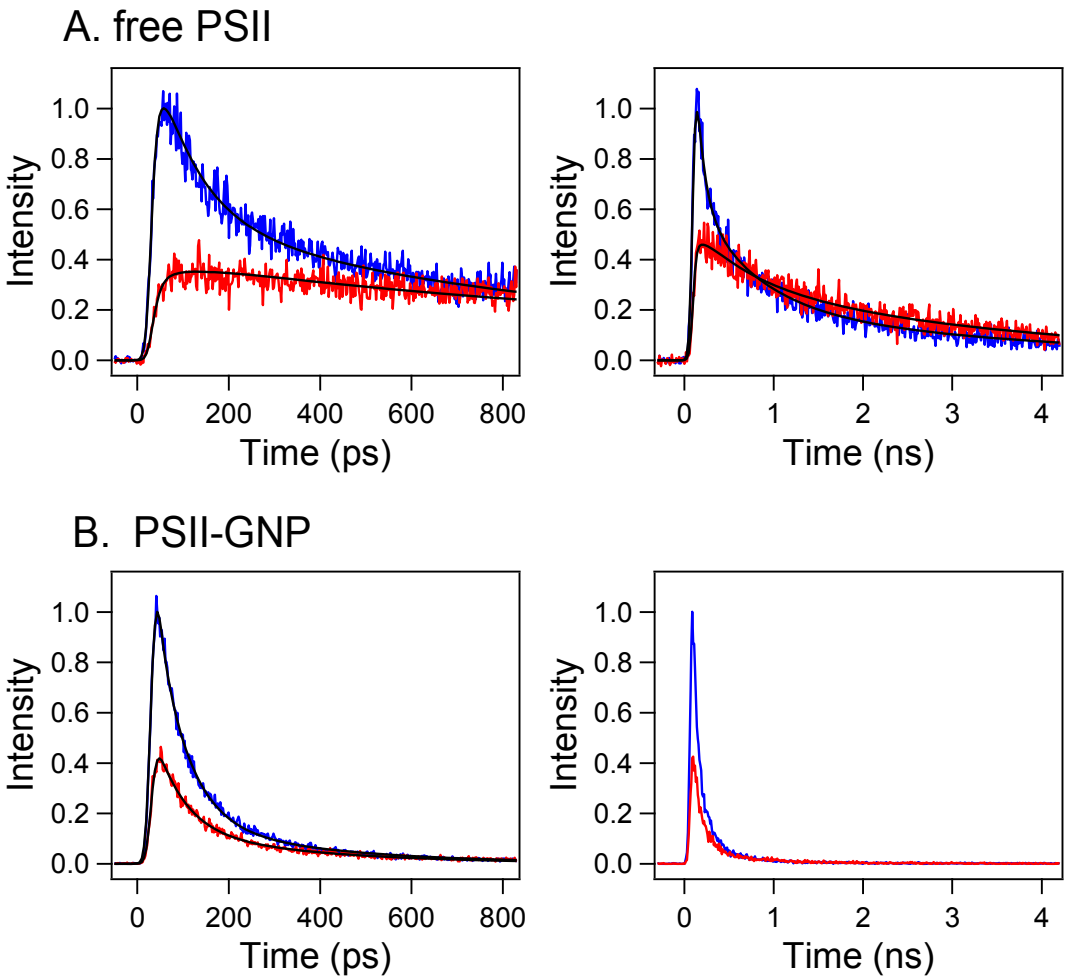
A. free PSII
Intensity
1.0
0.8
0.6
0.4
0.2
0.0
0
200
400
600
800
Time (ps)
Intensity
1.0
0.8
0.6
0.4
0.2
0.0
0
1
2
3
4
Time (ns)
B. PSII-GNP
Intensity
1.0
0.8
0.6
0.4
0.2
0.0
0
200
400
600
800
Time (ps)
Intensity
1.0
0.8
0.6
0.4
0.2
0.0
0
1
2
3
4
Time (ns)

Figure 5

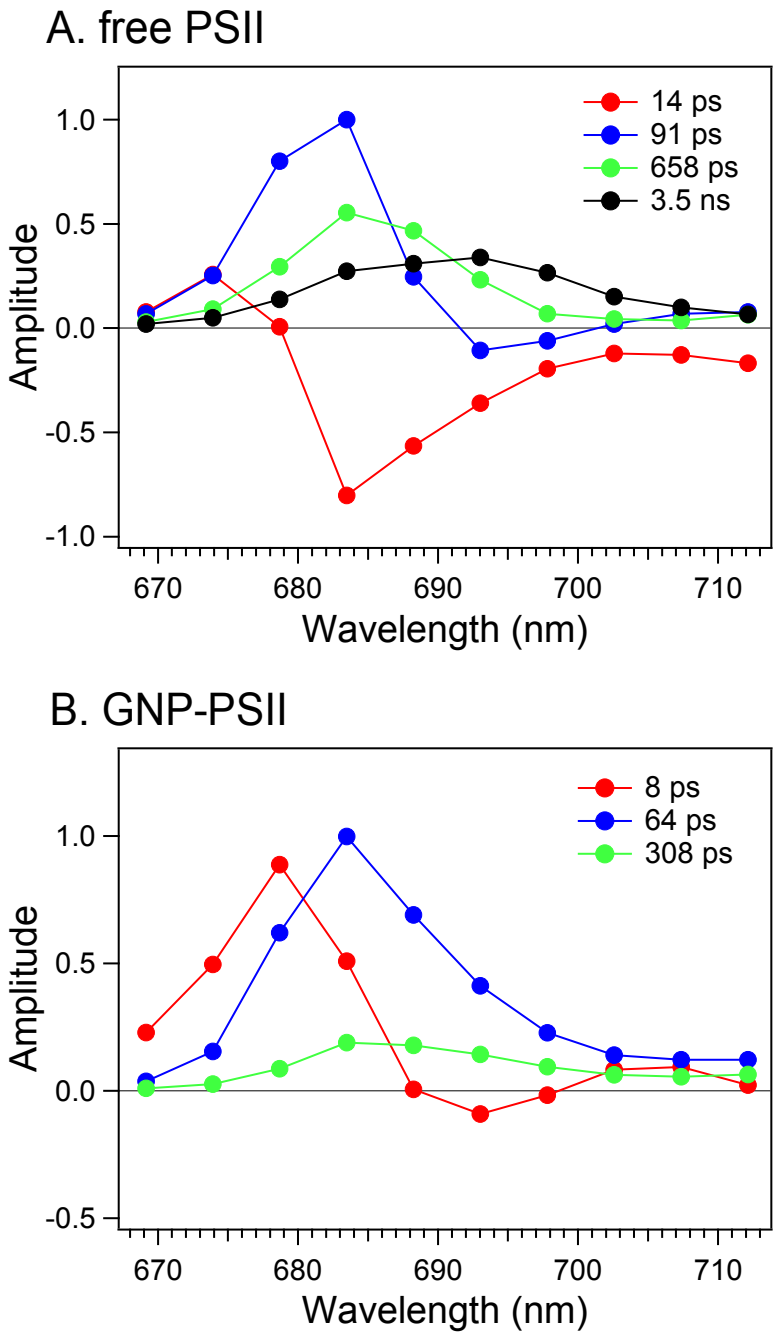
A. free PSII
14 ps
91 ps
658 ps
3.5 ns
1.0
0.5
0.0
-0.5
-1.0
Amplitude
670
680
690
700
710
Wavelength (nm)
B. GNP-PSII
8 ps
64 ps
308 ps
1.0
0.5
0.0
-0.5
Amplitude
670
680
690
700
710
Wavelength (nm)

Figure 6

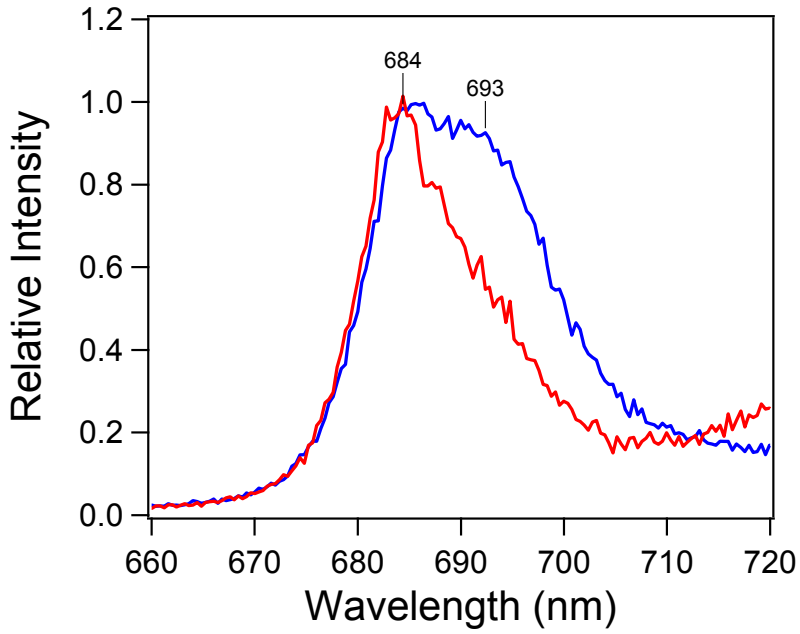
1.2
1.0
0.8
0.6
0.4
0.2
0.0
Relative Intensity
684
693
660
670
680
690
700
710
720
Wavelength (nm)

Figure 7

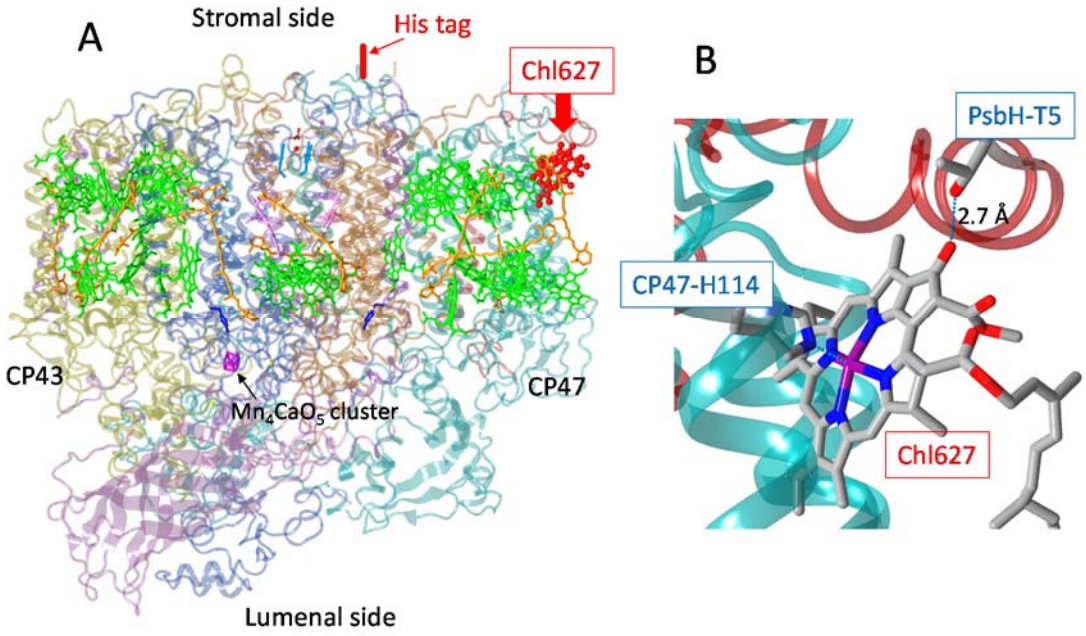
A
Stromal side
His tag
Chl627
CP43
CP47
Mn_4CaO_5 cluster
Lumenal side
B
PsbH-T5
2.7 Å
CP47-H114
Chl627

Figure 8